British Journal of Nutrition (2011), **105**, 1607–1618
doi:10.1017/S000711451000526X

Absorption and metabolism of olive oil secoiridoids in the small intestine

Joana Pinto[1,2], Fátima Paiva-Martins[1], Giulia Corona[2], Edward S. Debnam[3], Maria Jose Oruna-Concha[2], David Vauzour[2], Michael H. Gordon[2] and Jeremy P. E. Spencer[2]*

[1]*CIQ, Departamento de Química, Faculdade de Ciências da Universidade do Porto, Rua do Campo Alegre, 687 Porto, Portugal*
[2]*Molecular Nutrition Group, School of Chemistry, Food and Pharmacy, University of Reading, PO Box 226, Reading RG6 6AP, UK*
[3]*Department of Neuroscience, Physiology and Pharmacology, University College London, Royal Free Campus, London NW3 2PF, UK*

(Received 12 July 2010 – Revised 9 November 2010 – Accepted 16 November 2010 – First published online 17 March 2011)

Abstract

The secoiridoids 3,4-dihydroxyphenylethanol-elenolic acid (3,4-DHPEA-EA) and 3,4-dihydroxyphenylethanol-elenolic acid dialdehyde (3,4-DHPEA-EDA) account for approximately 55% of the phenolic content of olive oil and may be partly responsible for its reported human health benefits. We have investigated the absorption and metabolism of these secoiridoids in the upper gastrointestinal tract. Both 3,4-DHPEA-EDA and 3,4-DHPEA-EA were relatively stable under gastric conditions, only undergoing limited hydrolysis. Both secoiridoids were transferred across a human cellular model of the small intestine (Caco-2 cells). However, no glucuronide conjugation was observed for either secoiridoid during transfer, although some hydroxytyrosol and homovanillic alcohol were formed. As Caco-2 cells are known to express only limited metabolic activity, we also investigated the absorption and metabolism of secoiridoids in isolated, perfused segments of the jejunum and ileum. Here, both secoiridoids underwent extensive metabolism, most notably a two-electron reduction and glucuronidation during the transfer across both the ileum and jejunum. Unlike Caco-2 cells, the intact small-intestinal segments contain NADPH-dependent aldo-keto reductases, which reduce the aldehyde carbonyl group of 3,4-DHPEA-EA and one of the two aldeydic carbonyl groups present on 3,4-DHPEA-EDA. These reduced forms are then glucuronidated and represent the major *in vivo* small-intestinal metabolites of the secoiridoids. In agreement with the cell studies, perfusion of the jejunum and ileum also yielded hydroxytyrosol and homovanillic alcohol and their respective glucuronides. We suggest that the reduced and glucuronidated forms represent novel physiological metabolites of the secoiridoids that should be pursued *in vivo* and investigated for their biological activity.

Key words: 3,4-Dihydroxyphenylethanol-elenolic acid dialdehyde: 3,4-Dihydroxyphenylethanol-elenolic acid: Olive oil: Metabolism

Adherence to the so-called Mediterranean diet[1] is believed to provide protection against an array of common chronic pathological conditions, including CHD, cancer and neurodegenerative disorders[2–4]. These effects may be mediated by many individual components of the diet, including polyphenolic phytochemicals present in various fruits and vegetables, red wine and olive oil[4–6]. With regard to olive oil, these polyphenols include phenyl alcohols, such as hydroxytyrosol (HT), tyrosol and secoiridoids, and phenyl alcohols conjugated to elenolic acid. In particular, olive oil is a rich source of oleuropein aglycone, 3,4-dihydroxyphenylethanol-elenolic acid (3,4-DHPEA-EA, HT linked to elenolic acid) and a related compound 3,4-dihydroxyphenylethanol-elenolic acid dialdehyde (3,4-DHPEA-EDA, HT linked to the dialdehydic form of elenolic acid)[7] (Fig. 1). These compounds account for up to 55% of the total phenolic fraction[8–10], with 3,4-DHPEA-EDA and 3,4-DHPEA-EA achieving a relatively high concentration depending on growing conditions, cultivar and storage conditions[9,10]. These secoiridoid aglycones, together with other phenolic components and tocopherols, are believed to be partly responsible for the observed health benefits of extra virgin olive oil consumption[5,6].

Abbreviations: 3,4-DHPEA-EA, 3,4-dihydroxyphenylethanol-elenolic acid; 3,4-DHPEA-EAH$_2$, methyl 4-(2-(3,4-dihydroxyphenethoxy)-2-oxoethyl)-3-(hydroxymethyl)-2-methyl-3,4-dihydro-2*H*-pyran-5-carboxylate; 3,4-DHPEA-EDA, 3,4-dihydroxyphenylethanol-elenolic acid dialdehyde; 3,4-DHPEA-EDAH$_2$, 2-(3,4-dihydroxyphenyl)ethyl (4*E*)-4-formyl-3-(2-hydroxyethyl)hex-4-enoate; AP, apical; BA, basolateral; ECACC, European Collection of Cell Culture; HT, hydroxytyrosol; HVA, homovanillyl alcohol; LC, liquid chromatography; RT, retention time.

* **Corresponding author:** Dr J. P. E. Spencer, email j.p.e.spencer@rdg.ac.uk

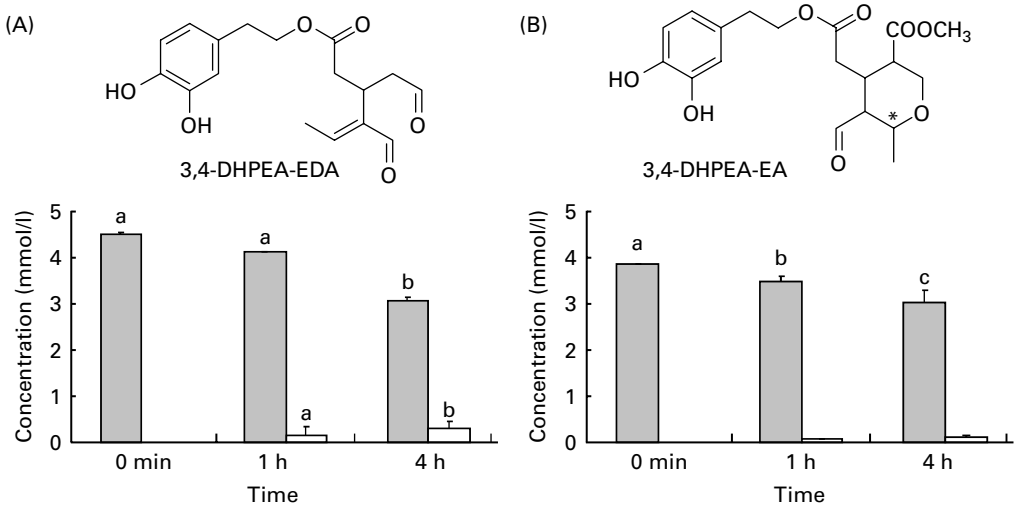

Fig. 1. Structures and amounts of olive oil secoiridoids under study obtained after the incubation of compounds at 37°C, pH 2. (A) ■, 3,4-Dihydroxyphenylethanol-elenolic acid dialdehyde (3,4-DHPEA-EDA); □, hydroxytyrosol. (B) ■, 3,4-Dihydroxyphenylethanol-elenolic acid (3,4-DHPEA-EA); □, hydroxytyrosol. Values are means of at least four separate experiments, with standard errors represented by vertical bars. [a,b,c] Mean values with unlike letters were significantly different ($P<0·05$).

In vitro studies have indicated that 3,4-DHPEA-EDA and 3,4-DHPEA-EA may protect erythrocytes[11,12] and mononuclear cells[13] against oxidative injury. Furthermore, they are known to reduce the viability of human breast carcinoma cells[14] and induce apoptosis in mammary epithelial cells overexpressing human epidermal growth factor receptor-2[15] via the modulation of human epidermal growth factor receptor-2 auto-phosphorylation[16]. However, the biological properties of 3,4-DHPEA-EDA and 3,4-DHPEA-EA *in vivo* will depend on the extent to which they are absorbed and metabolised in the gastrointestinal tract. Absorption studies with olive oil, or phenolic extracts derived from olive oil, have indicated that HT is absorbed[17–22], while other phenolic components undergo metabolism in the small and large intestine to yield homovanillic acid and homovanillyl alcohol (HVA)[23–25]. For example, oleuropein (3,4-DHPEA-EA glucoside) is not absorbed in the small intestine, but undergoes rapid degradation in the large intestine to yield HT[23]. However, unlike oleuropein, it is thought that its corresponding aglycone (3,4-DHPEA-EA) may be absorbed in the small intestine due to its higher partition coefficient (log *p*) value[26,27]. As such, the aim of the present study was to investigate the absorption and metabolism of the secoiridoids 3,4-DPEA-EA and 3,4-DHPEA-EDA in the small intestine. We focus on their decomposition in the stomach and their absorption and metabolism in two small-intestinal models in order to acquire knowledge relating to their fate in the gastrointestinal tract and the generation of metabolites that may exert potential bioactivity *in vivo*.

Experimental methods

Materials

The aglycone 3,4-DHPEA-EA was obtained from oleuropein via enzymatic cleavage using β-glycosidase (Fluka, Buchs, Switzerland)[28], while 3,4-DHPEA-EDA was extracted from olive leaves, as described previously[29]. 3,4-DHPEA-EA that was isolated following β-glycosidase treatment was found to consist of a mixture of approximately 3·7:6·3 of its *cis*- and *trans*-isomers. The purity of both compounds was assessed by liquid chromatography (LC)–MS and ^{1}H NMR and was determined to be more than 95% pure. HT was purchased from Cayman Chemical Company (Ann Arbor, MI, USA). HVA and β-glucuronidase (type L-II from limpets) were purchased from Sigma (Poole, Dorset, UK). The Caco-2 cell line was obtained from the European Collection of Cell Cultures (ECACC) (Salisbury, Wiltshire, UK). Cell culture media and supplements were obtained from PAA Laboratories (Yeovil, Somerset, UK). HPLC-grade solvents were obtained from Fisher (Hampton, NH, USA), and HPLC columns were obtained from Waters (Watford, Herts, UK). All other reagents used were obtained from Sigma.

Low pH conditions

3,4-DHPEA-EDA or 3,4-DHPEA-EA (1 mM) was incubated in simulated gastric pH conditions (water and HCl; pH 2) at 37°C for 1 and 4 h. As the aqueous system had no inherent buffering capacity, we monitored pH throughout incubations in order to assess whether compound hydrolysis influences pH. However, there was no significant change in pH during any of the incubations. Following incubation, samples were analysed by HPLC-diode-array detection (see later).

Transport experiments using human Caco-2 cells

Caco-2 cells (passage 25–40) were grown in T-75 culture flasks and passaged with a trypsin–versene solution. Cells were cultured in Dulbecco's modified Eagle's medium supplemented with fetal bovine serum (20%, v/v), non-essential amino acids (1%, v/v), L-glutamine (2 mM), penicillin (100 units/ml) and streptomycin (100 μg/ml) at 37°C in 5% CO_2. For all transcellular transport studies, Caco-2 cells were

seeded in 12 mm internal diameter transwell inserts (polycarbonate membrane, 0·4 μm pore size; Corning Costar Corporation, Cambridge, MA, USA) in twelve-well plates at a density of 5×10^4 cells/ml. The basolateral (BA, serosal) and apical (AP, mucosal) compartments contained 1·5 and 0·5 ml of the culture medium, respectively. The culture medium was replaced three times a week for 21 d. Before transport experiments, the media in both chambers were replaced with HEPES-buffered medium (pH 7·4; 5 mM-HEPES, 154 mM-NaCl, 4·6 mM-KCl, 33 mM-glucose, 5 mM-$NaHCO_3$ and 1·2 mM-Na_2HPO_4). Only inserts with a transepithelial electrical resistance value of $>300\,\Omega/cm^2$ were used for transport experiments. 3,4-DHPEA-EA or 3,4-DHPEA-EDA (50, 100 and 200 μM) was added in the AP side of transwells and incubated for 2 h. Following incubation, the medium from both compartments was harvested, snap-frozen and was analysed by HPLC. Control experiments to monitor the oxidation and hydrolysis of both compounds in medium alone (i.e. in the absence of cells) were performed. In control experiments, DHPEA-EA and 3,4-DHPEA-EDA were observed to undergo only a very small level of spontaneous degradation to yield HT (2 h, 37°C; data not shown).

Transport and metabolism experiments in the perfused rat intestinal model

Transport and metabolism experiments were conducted using the *in vitro* intestinal preparation of Fisher & Gardner[30,31], in which the lumen of the isolated intestine is perfused with a segmental flow (perfusion of buffer interspersed with the gas mixture) of bicarbonate buffer (pH 7·4) equilibrated with 95 % O_2:5 % CO_2 and containing 28 mM-glucose. The bicarbonate buffer consisted of 25 mM-HCO_3^-, 143 mM-Na^+, 133·7 mM-Cl^-, 5·9 mM-K^+, 1·2 mM-HPO_4^-, 2 mM-Ca^{2+} and 1·2 mM-Mg^{2+}. Male Sprague–Dawley rats (230–260 g) were anaesthetised with sodium pentobarbital (90 mg/kg, intraperitoneally), and sections of the jejunum (20–30 cm long, beginning 10 cm from the ligament of Treitz) or ileum (20–30 cm long, ending 5 cm from the ileo-caecal junction) were cannulated, and the lumen was segmentally perfused. The intestinal sections were then removed from the animal by stripping them from the mesentery, and suspended in a chamber containing liquid paraffin (37°C). Segmental flow was maintained throughout this procedure. Before transport experiments, the segments were perfused for 40 min in order to flush blood from the vasculature and to allow fluid absorption to reach a steady state. Thereafter, an aliquot of the methanol stock solution of 3,4-DHPEA-EA or 3,4-DHPEA-EDA was added to the carbonate buffer (final concentration 100 μM, methanol content 0·1 %) and perfused through the intestinal segment, in a single-pass fashion, for up to 80 min. Appropriate vehicle controls, lacking polyphenols, were also conducted. During perfusion, absorbed fluid dropped through the paraffin to the base of the chamber and was collected at timed intervals of 20 min. All samples (pre-perfusion, post-perfusion and timed serosal fluids) were snap-frozen and stored at −20°C until analysis. Serosal fluid samples were analysed by HPLC and LC–MS both pre- and post-β-glucuronidase treatment to establish the presence of glucuronide conjugates. Aliquots of serosal fluid samples (100 μl) were added to 50 μl of phosphate buffer (final concentration 0·1 M; pH 4·5) with or without the glucuronidase enzyme (2000 units/ml), and samples were incubated for 120 min at 37°C. The 0·1 M-phosphate buffer effectively inhibits all sulphatase activity that the enzyme possesses. After incubation, samples were centrifuged at 13 200 rpm for 10 min, and aliquots of the supernatant were used for HPLC and LC–MS analysis.

HPLC analysis

Characterisation and quantification of phenolic components and metabolites in serosal samples and cell medium samples were carried out using a Hewlett-Packard 1100 series liquid chromatography system (Hewlett-Packard, Palo Alto, CA, USA) equipped with a diode array detector (HP ChemStation Software system). Samples were analysed by reverse-phase HPLC using a Nova-Pak C18 column ($4·6 \times 250\,mm^2$) with 4 μm particle size. The temperature of the column was maintained at 30°C. The mobile phases consisted of a mixture of aqueous methanol (5 %) in 0·1 % 5M-HCl (A) and a mixture of aqueous acetonitrile (50 %) in 0·1 % 5M-HCl (B) and were pumped through the column at 0·7 ml/min. The following gradient system was used (min/% B): 0/5, 5/5, 40/50, 55/100, 59·9/100, 60/5, with 10 min post-run for both compound and metabolite detections. The eluent was monitored by photodiode array detection at 280 nm, and spectra of products were obtained over the 200–600 nm range. Calibration curves of the compounds (0·1–100 μM) were constructed using authentic standards (HT, HVA, 3,4-DHPEA-EA and 3,4-DHPEA-EDA), and in each case, they were found to be linear with correlation coefficients higher than 0·992. Quantification of glucuronides (i.e. following β-glucuronidase treatment) and reduced derivatives of 3,4-DHPEA-EA and 3,4-DHPEA-EDA was achieved using 3,4-DHPEA-EA and 3,4-DHPEA as standards.

Liquid chromatography–mass spectrometry analysis

Metabolite characterisation was achieved using LC–MS/MS utilising electrospray ionisation. This consisted of an Agilent 1200 HPLC system equipped with a binary pump, degasser, autosampler, thermostat, column heater, photodiode array detector and an Agilent 1100 Series LC/MSD mass trap spectrometer. Separation of samples was achieved using a Zorbax SB C18 column ($2·1 \times 100\,mm^2$; 1·8 μm; Agilent, Santa Clara, CA, USA), and HPLC conditions were as follows: injection volume, 1 μl; column temperature, 25°C; binary mobile system: (A) 0·1 % of aqueous formic acid and (B) 0·1 % of formic acid in acetonitrile; flow rate, 0·2 ml/min. A series of linear gradients was used for separation (min/%B): 0/10, 3/10, 15/40, 40/70, 50/70 and 65/10. MS was performed in the negative ion mode (scan range, m/z 100–800 Da; source temperature, 350°C). All solvents used were of LC–MS grade.

British Journal of Nutrition

Statistical analysis

Statistical analyses were performed using SPSS 18 statistical software (SPSS, Inc., Chicago, IL, USA). Results are reported as means with their standard errors of at least three separated experiments. Data were analysed by one-way ANOVA followed by the Tukey–Duncan α *post hoc* test, and differences were considered significant at $P<0{\cdot}05$. The Pearson correlation coefficient (R) was used to indicate the strength of a linear relationship. A P value lower than 0·05 was considered as evidence that the null hypothesis is false, and the attributes were statistically significantly correlated.

Results and discussion

Incubation at low pH

Incubation of 3,4-DHPEA-EDA and 3,4-DHPEA-EA at pH 2·0 led to the partial hydrolysis of both compounds and a corresponding time-dependent increase in HT (Fig. 1). After 4 h incubation, about 67 % of 3,4-DHPEA-EDA and 78 % of 3,4-DHPEA-EA (Fig. 1(A) and (B)) remained. The present results show that although some hydrolysis takes place releasing free HT from both 3,4-DHPEA-EDA and 3,4-DHPEA-EA, a large amount of both DHPEA-EDA and 3,4-DHPEA-EA (67 and 78 %, respectively, after 4 h) remains intact despite prolonged exposure to postprandial gastric conditions. This is in agreement with previous studies, which suggest that both compounds are also relatively stable at pH environments akin to those in the small intestine with more than 90 % of 3,4-DHPEA-EDA and more than 65 % of 3,4-DHPEA-EA remaining intact after a 48 h incubation at pH 7·4 (37°C)[32]. These data suggest that both 3,4-DHPEA-EDA and 3,4-DHPEA-EA may be relatively stable during transit through the stomach and the small intestine *in vivo*. As a consequence, both compounds are likely to arrive at relatively high concentration in the small intestine where they may undergo absorption and metabolism.

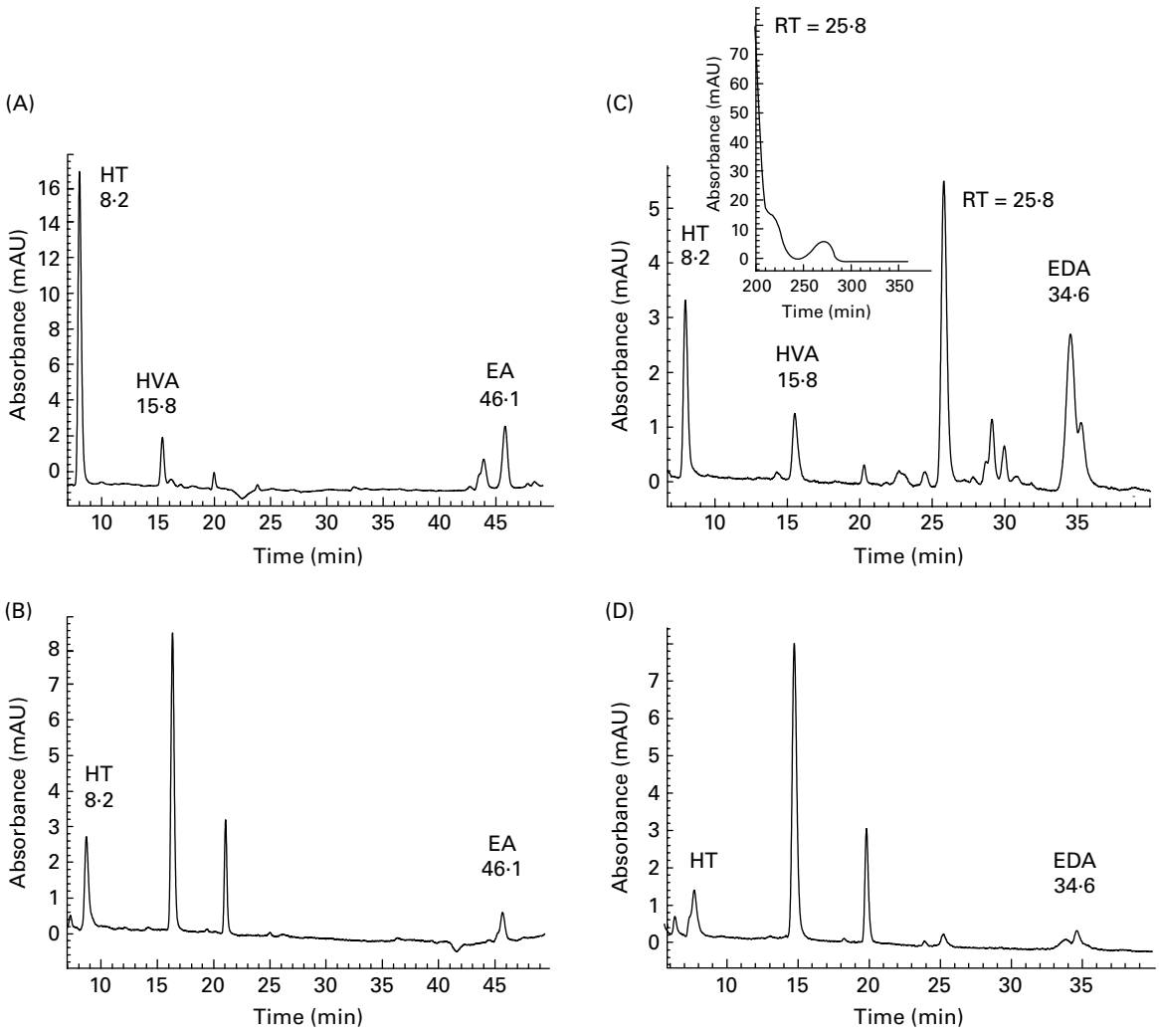

Fig. 2. HPLC chromatogram with photodiode array detection (200–600 nm) of the cell culture apical (A, C) and basolateral (B, D) buffer from Caco-2 monolayers after 2 h incubation with 3,4-dihydroxyphenylethanol-elenolic acid (3,4-DHPEA-EA) (A, B) and 3,4-dihydroxyphenylethanol-elenolic acid dialdehyde (3,4-DHPEA-EDA) (C, D) at 100 mM. Detection was performed at 280 nm. HT, hydroxytyrosol; HVA, homovanillyl alcohol; EA, 3,4-DHPEA-EA; RT, retention time; EDA, 3,4-DHPEA-EDA.

Caco-2 cell model

Initial investigations into the ability of 3,4-DHPEA-EA and 3,4-DHPEA-EDA to transfer across the small intestine were conducted using the human Caco-2 cell model. Analysis of the AP and BA medium demonstrated the enterocyte-mediated transfer of both 3,4-DHPEA-EA and 3,4-DHPEA-EDA over a 2 h period (Fig. 2). After 2 h, the *cis*- and *trans*-isomers of 3,4-DHPEA-EA (retention time (RT): 44·6 and 46·1 min) were detectable on the AP side (Fig. 2(A)), and a single isomer was detected on the BA side of the cell monolayer (Fig. 2(B)). Furthermore, its transfer to the BA side was observed to increase with increasing exposure to the AP side (Fig. 3(A), I–III). HT (RT: 8·2 min) was also detected on both the AP and BA sides (Figs. 2 and 3), whereas HVA (RT: 15·8 min) was only detected on the AP side. Similarly, 3,4-DHPEA-EDA appeared to be transferred from the AP side (Fig. 2(C)) to the BA side (Fig. 2(D)) in a concentration-dependent manner (Fig. 3(B), I–III), where HT (RT: 8·2 min) was also found. LC–MS of BA fluids confirmed the identity of 3,4-DHPEA-EA and 3,4-DHPEA-EDA, indicating that they appear to be capable of enterocytic transfer. LC–MS of the AP medium following 3,4-DHPEA-EDA exposure (Fig. 2(C)) indicated the presence of HVA (RT: 15·8; m/z 153) and another intense peak (RT: 25·8 min), which apparently had a molecular peak of $m/z = 250$ (other fragments: $m/z = 220$ and 198). The peaks at 16·1 and 21·9 min on the BA side were compounds related to normal enterocyte metabolism, were present in controls and therefore we did not characterise them.

These data appear to suggest that both 3,4-DHPEA-EA and 3,4-DHPEA-EDA are transferred across the small intestine. However, while Caco-2 cell monolayers have been shown to express a series of metabolic enzymes and efflux transporters[33,34], they are well known to overexpress some enzymes and underexpress others. Although the Caco-2 cell model is generally considered to be a suitable model for intestinal CYP3A4-mediated first-pass metabolism, this is not the case for (uridine 5′-diphospho-glucuronosyl transferase)-mediated glucuronidation[35,36], as they do not contain a full complement of intestinal drug-metabolising enzymes. However,

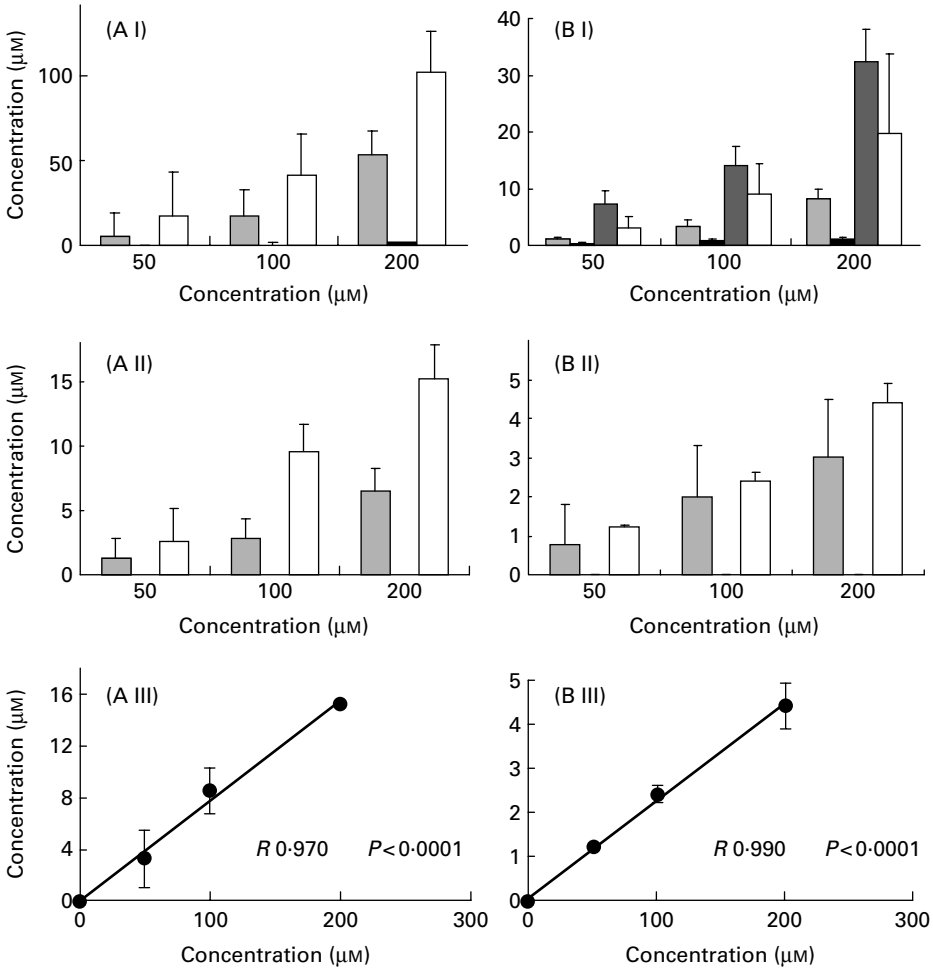

Fig. 3. Amount of (A) 3,4-dihydroxyphenylethanol-elenolic acid and (B) 3,4-dihydroxyphenylethanol-elenolic acid dialdehyde and their metabolites after 2 h incubation in the cell culture (I) apical and (II) basolateral buffer and (III) concentration dependence of polyphenol transport in Caco-2 cells. Values are means of at least four separate experiments, with standard errors represented by vertical bars. The Pearson correlation coefficient (R) was used to indicate the strength of a linear relationship. A P value lower than 0·05 was considered as evidence that the null hypothesis is false and the attributes were statistically significantly correlated. ▨, Hydroxytyrosol; ■, homovanillyl alcohol; ▩, retention time (25·8 min); □, secoiridoid.

they have been extensively used for assessing the small-intestinal absorption and metabolism of polyphenols[24,37–39], even though this cell system may not wholly reflect physiological conditions *in vivo*. For example, several enzymes involved in lipid and carbohydrate metabolism are overexpressed relative to the human intestinal epithelial cells[33], whereas uridine 5′-diphospho-glucuronosyl transferase[40], catechol-*O*-methyl transferase, aldolase and retinal dehydrogenase[33] are underexpressed. As such, the results obtained from our cell studies may not fully reflect the degree to which 3,4-DHPEA-EA and 3,4-DHPEA-EDA undergo enterocytic metabolism *in vivo*. Furthermore, the reduced metabolic capacity of these cells may result in an incomplete picture of the actual pattern of 3,4-DHPEA-EA and 3,4-DHPEA-EDA absorption and metabolism, most notably whether the parent compounds are transferred intact in the presence of enterocytes with a normal metabolic capacity.

Perfused rat intestinal model

To help address this problem, we also carried out transfer experiments in the isolated, perfused rat intestinal model, which is known to possess full metabolic capacity for up to 120 min post-isolation[30,31]. Using this model, we were able to determine the comparative absorption of 3,4-DHPEA-EA and DHPEA-EDA, and the extent to which they are conjugated and metabolised during transfer across the jejunum and ileum. HPLC analysis of the serosal fluid (equivalent to the portal vein blood) following perfusion of the ileum with 3,4-DHPEA-EA led to the detection of a number of peaks (Fig. 4), which were characterised by diode array and MS. These included HT (RT: 8·4 min; *m/z* 153), 3-*O*-methyl-HT (HVA) (RT: 16·5 min; *m/z* 153), HT glucuronide (RT: 6·8; *m/z* 329) and HVA glucuronide (RT: 11·5; *m/z* 343) (Fig. 4(A)). In addition, there were two peaks at 44·6 and 45·5 min that had similar, but not identical, spectral and RT characteristics

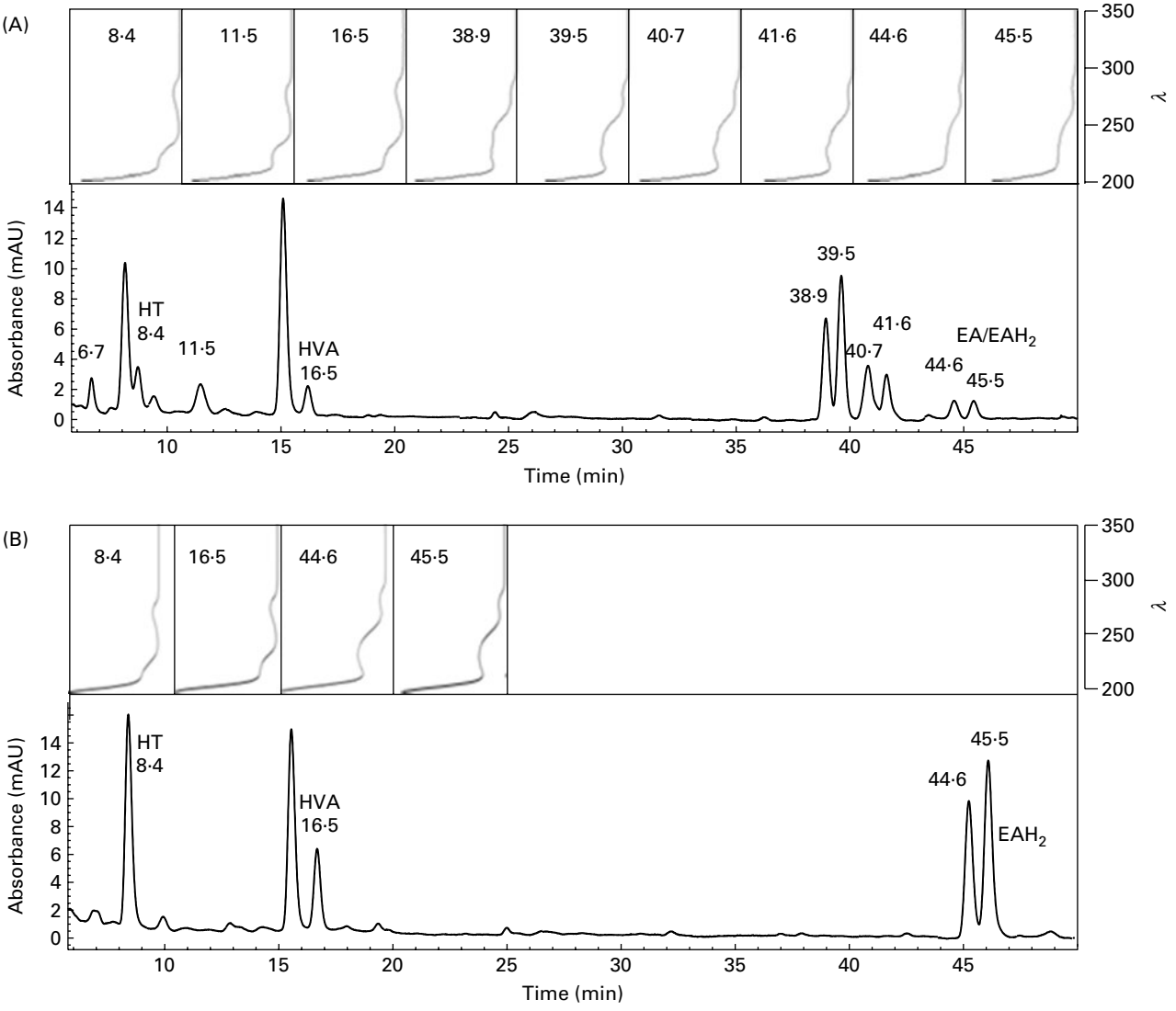

Fig. 4. HPLC chromatogram with photodiode array detection (200–350 nm) of the absorbed fluid after 3,4-dihydroxyphenylethanol-elenolic acid (3,4-DHPEA-EA) perfusion through the isolated rat ileum. (A) Absorbed fluid and (B) absorbed fluid treated with β-glucuronidase. Detection was performed at 280 nm. HT, hydroxytyrosol; HVA, homovanillyl alcohol; EA, 3,4-DHPEA-EA; EAH_2, reduced 3,4-DHPEA-EA.

to the *cis*- and *trans*-isomers of 3,4-DHPEA-EA and a further four peaks at a RT between 38 and 43 min (Fig. 4(A)). MS analysis indicated that the four peaks at 38–43 min had a + 2 mass (*m/z* 555; negative ion mode) relative to that of 3,4-DHPEA-EA glucuronide, indicating that they were glucuronides of reduced forms of the *cis*- and *trans*-isomers of 3,4-DHPEA-EA (Fig. 5). β-Glucuronidase treatment confirmed that these were indeed glucuronides (Fig. 4(A)), and MS analysis of the peaks at 44·6 and 45·5 min, which appeared following enzyme treatment (Fig. 4(B)), was shown to correspond to the reduced *cis*- and *trans*-isomers of 3,4-DHPEA-EA (denoted as methyl 4-(2-(3,4-dihydroxyphenethoxy)-2-oxoethyl)-3-(hydroxymethyl)-2-methyl-3,4-dihydro-2*H*-pyran-5-carboxylate (3,4-DHPEA-EAH$_2$); molecular ion in negative mode of *m/z* = 379 for both peaks). We were unable to confirm the identity of the peaks at 44·6 and 45·5 min (Fig. 4(A)) due to the small amounts transferred, although these are likely to correspond either to 3,4-DHPEA-EA or its reduced derivatives. Therefore, the quantification of these peaks was denoted as EA/EAH$_2$ and quantified as 3,4-DHPEA-EA equivalents.

These results indicate that during transfer across the ileum, 3,4-DHPEA-EA undergoes both a two-electron reduction to yield 3,4-DHPEA-EAH$_2$ and mono-glucuronidation at two positions. Two sites of reduction are possible on 3,4-DHPEA-EA, the alkenic double bond and the carbonyl group (Fig. 1(B)), which may act as sites for the action of NADPH-dependent,

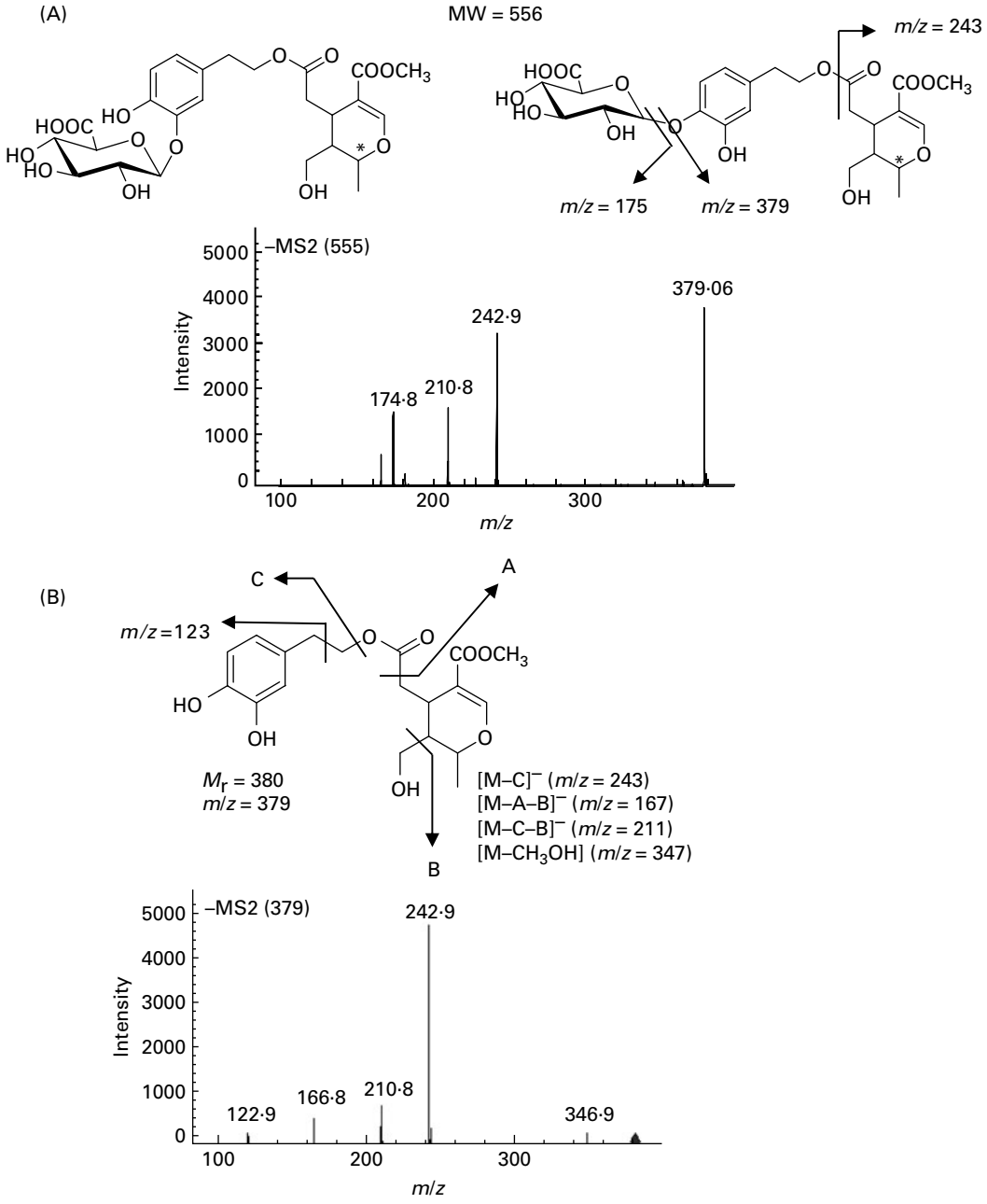

Fig. 5. MS/MS (MS2) negative fragment ion spectrum of (A) *m/z* 555 (reduced 3,4-dihydroxyphenylethanol-elenolic acid (3,4-DHPEA-EA) glucuronides) and (B) *m/z* 379 (reduced 3,4-DHPEA-EA) and proposed fragmentation. MW, molecular weight.

aldo-keto reductase[41]. Aldo-keto reductase enzymes are widely distributed in mammals and include human aldose reductase and human small intestine aldose reductase[42]. These enzymes are capable of catalysing the reduction of a variety of carbonyl-containing compounds, and are responsible for the reduction of retinal to retinol in the human small intestine[42], as well as the reduction of various other molecules, including carbohydrates, aliphatic and aromatic aldehydes and steroids. We suggest that during transfer across enterocytes, aldose reductase reduces the carbonyl group of 3,4-DHPEA-EA, something that was consistent with the MS fragmentation pattern of 3,4-DHPEA-EAH$_2$ (Fig. 5). Although we were unable to completely rule out the transfer of 3,4-DHPEA-EA, it appears that its major bioavailable forms *in vivo* are the glucuronides of reduced 3,4-DHPEA-EA (methyl 4-(2-(3,4-dihydroxyphenyl)-ethoxycarbonylmethyl)-3-hydroxymethyl-2-methyl-3,4-dihydro-2H-pyran-5-carboxylate). Presumably, we did not observe these in the cell model due to the underexpression of these enzymes.

Similar observations were made following perfusion of the ileum with 3,4-DHPEA-EDA (Fig. 6). HT (RT: 8·0 min), HVA (RT: 15·8 min) and the respective glucuronides of these compounds (RT: 7·6 and 11·8 min) were observed in the serosal fluid (Fig. 6(A)). In addition, there were two peaks at 30·7 and 32·1 min and a further peak at 34·4 min with a similar, but not identical, spectral and RT characteristics to 3,4-DHPEA-EDA. Full scan analysis of the serosal fluid collected after 3,4-DHPEA-EDA perfusion did not indicate the presence of the $[M - H]^-$ ion corresponding to 3,4-DHPEA-EDA (*m/z* 319) or to its reduced form (3,4-DHPEA-EDAH$_2$ (2-(3,4-dihydroxyphenyl)ethyl (4*E*)-4-formyl-3-(2-hydroxyethyl)hex-4-enoate), *m/z* 321). However, two glucuronides of the reduced form of 3,4-DHPEA-EDA were detected (RT: 30·7 and 32·1 min, *m/z* 497 in negative ion mode), which disappeared following β-glucuronidase treatment (Fig. 6(B)) with a subsequent increase in a peak at 34·4 min corresponding to a reduced form of 3,4-DHPEA-EDA (*m/z* 321 in negative ion mode). Again, the fragmentation of the molecular ion corresponding to 3,4-DHPEA-EDAH$_2$ (*m/z* 321) indicated that a reduction of one of the two carbonyl groups present on 3,4-DHPEA-EDA had occurred during transfer across the ileum (Fig. 7), along with glucuronidation. We were unable to

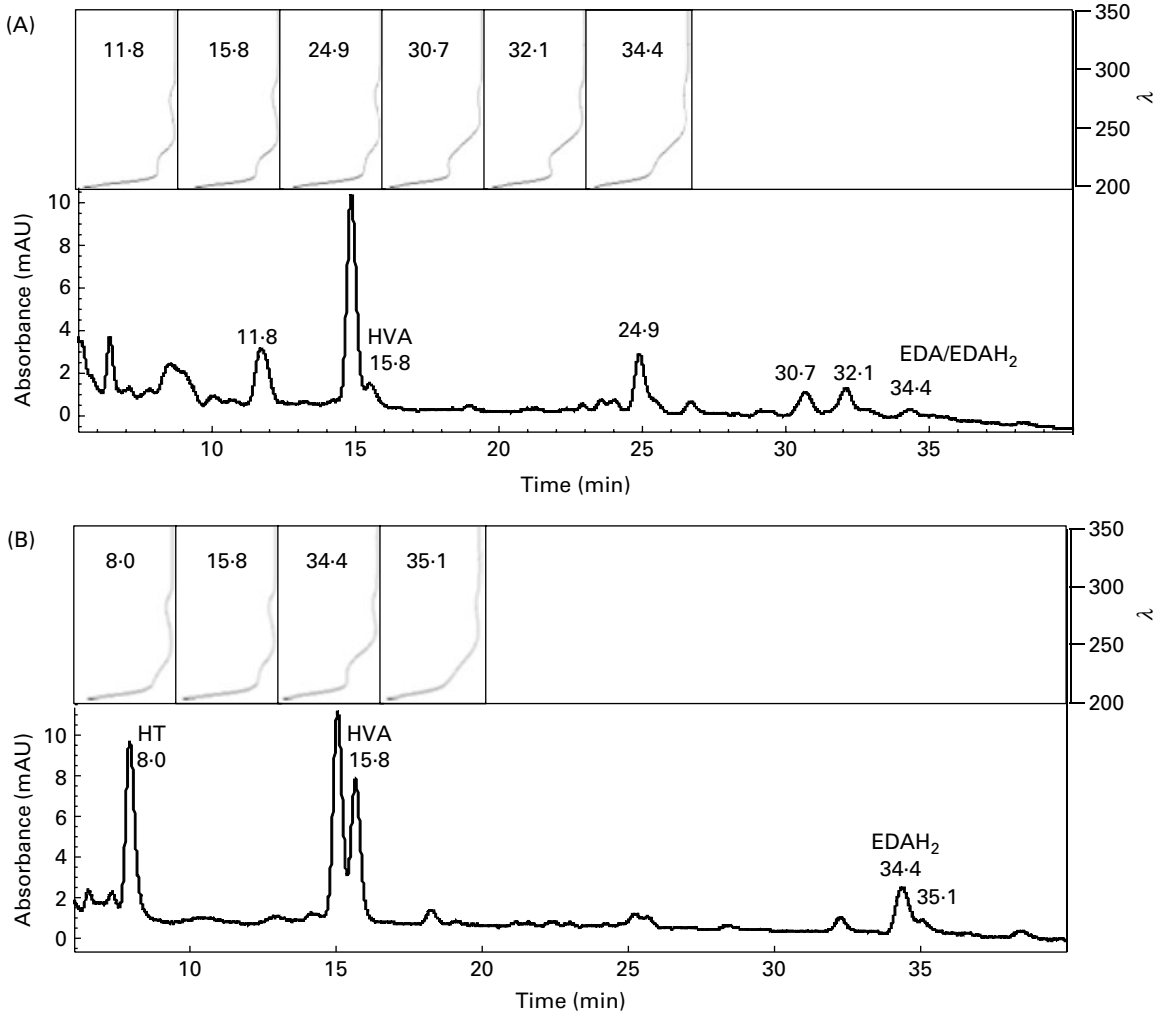

Fig. 6. HPLC chromatogram with photodiode array detection (200–350 nm) of the absorbed fluid after 3,4-dihydroxyphenylethanol-elenolic acid dialdehyde (3,4-DHPEA-EDA) perfusion through the isolated rat ileum. (A) Absorbed fluid and (B) absorbed fluid treated with β-glucuronidase. Detection was performed at 280 nm. HT, hydroxytyrosol; HVA, homovanillyl alcohol; EDA, 3,4-dihydroxyphenylethanol-elenolic acid; EDAH$_2$, reduced 3,4-DHPEA-EDA.

confirm which of the carbonyl functional groups had undergone reduction since reduction at either site would yield similar fragmentation patterns.

Perfusion of the jejunum with both 3,4-DHPEA-EDA and 3,4-DHPEA-EA also resulted in their extensive reduction and glucuronidation in a similar manner to that seen in the ileum. However, both 3,4-DHPEA-EDA and 3,4-DHPEA-EA metabolites were transferred to a greater extent in the jejunum compared with the ileum (Fig. 8(A)). This difference was especially apparent for 3,4-DHPEA-EA where the concentration of 3,4-DHPEA-EAH$_2$ glucuronide was four times higher in the jejunum serosal fluid than in the ileum serosal fluid. Furthermore, transfer of compounds and appearance of metabolites reached a maximum at about 60 min (Fig. 8(A) and (B)), reflecting the initial slow uptake of components into cells and followed by their enzymatic reduction and glucuronidation. The small reduction in compound/metabolite concentration in the jejunum at 90 min is likely to reflect a loss of viability in the intestinal segment at this late stage. There were also notable differences in the patterns of metabolism occurring between the jejunum and ileum, with ileum appearing to display a lower reductase and glucuronidase activity compared with the jejunum (Fig. 8). This is in agreement with previous studies indicating that the ileum expresses a

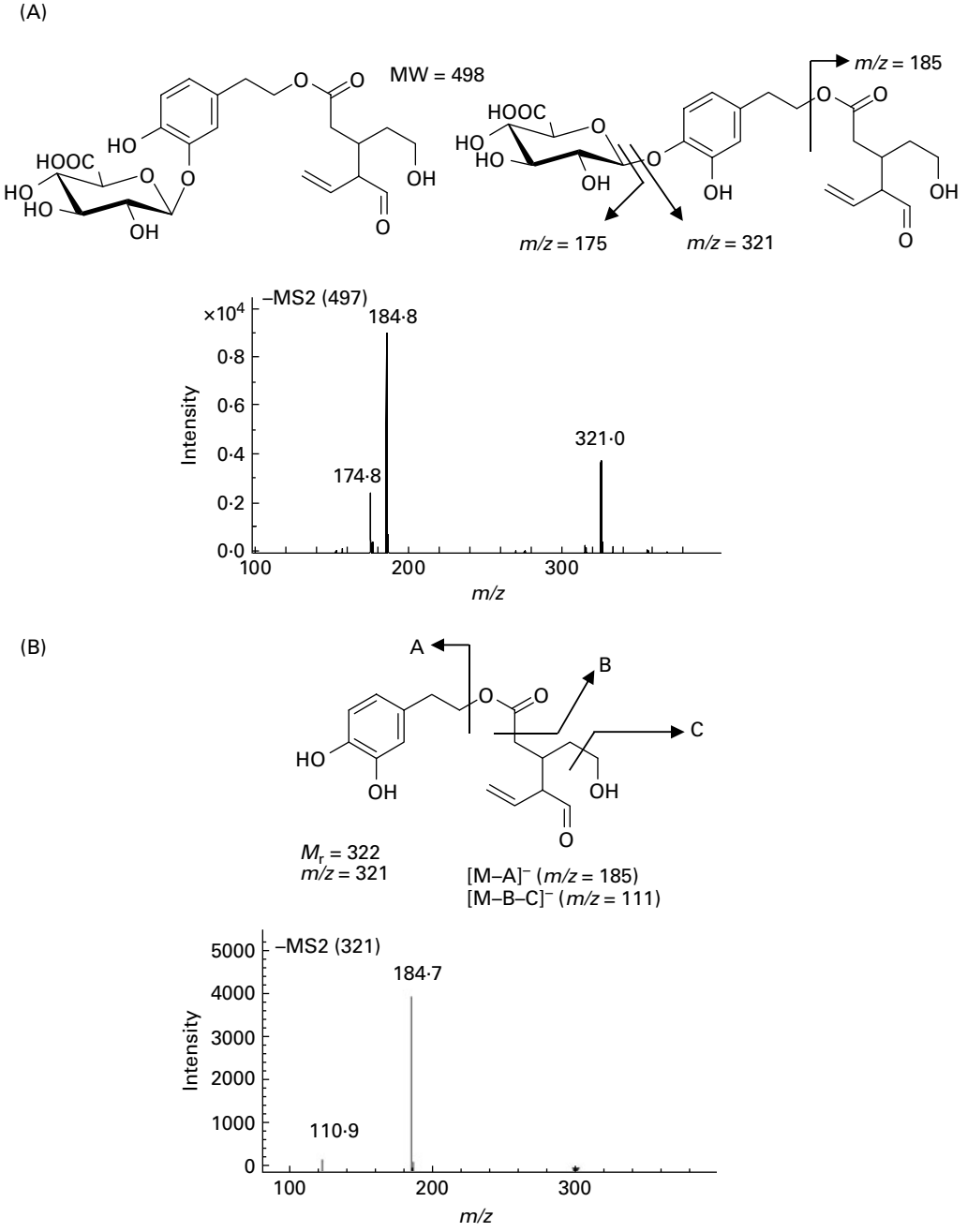

Fig. 7. MS/MS (MS2) negative fragment ion spectrum of (A) *m/z* 497 (reduced 3,4-dihydroxyphenylethanol-elenolic acid dialdehyde (3,4-DHPEA-EDA) glucuronides) and (B) *m/z* 321 (reduced 3,4-DHPEA-EDA) and proposed fragmentation.

much lower glucuronidase activity towards transferred flavonoids relative to the jejunum[31]. Nevertheless, when considering the small intestine as a whole, glucuronides of 3,4-DHPEA-EAH_2 and 3,4-DHPEA-$EDAH_2$ represent the major small-intestinal metabolites entering the portal blood.

Conclusion

Previous human intervention studies have failed to clearly identify 3,4-DHPEA-EA in either the plasma or urine following olive oil ingestion[19–21], while 3,4-DHPEA-EDA has only been measured in the plasma of one subject (out of five) in a recent study performed by Suarez *et al.*[43]. The inability to characterise and quantify these components may partially relate to a lack of commercially available secoiridoid standards and a focus on the detection of HT and tyrosol in biological samples. However, our data suggest that the inability to detect 3,4-DHPEA-EDA and 3,4-DHPEA-EA (or their glucuronides) in biological fluids is more likely to be due to the fact that they are not absorbed in the parental form, and thus they are not major bioavailable forms *in vivo*. Indeed, we show for the first time that the major small-intestinal metabolites of these secoiridoids are glucuronide conjugates of 3,4-DHPEA-EDA and 3,4-DHPEA-EA that have undergone reduction (most probably enzymatic) during enterocytic transfer. As such, previous studies are unlikely to have captured the full extent of absorption and metabolism of these olive oil components, as they would have failed to take account of these reduced forms. Therefore, it seems reasonable that previous human studies aimed at investigating the pharmacokinetics of such olive oil secoiridoids may have underestimated the full extent of their absorption. Future studies should take account

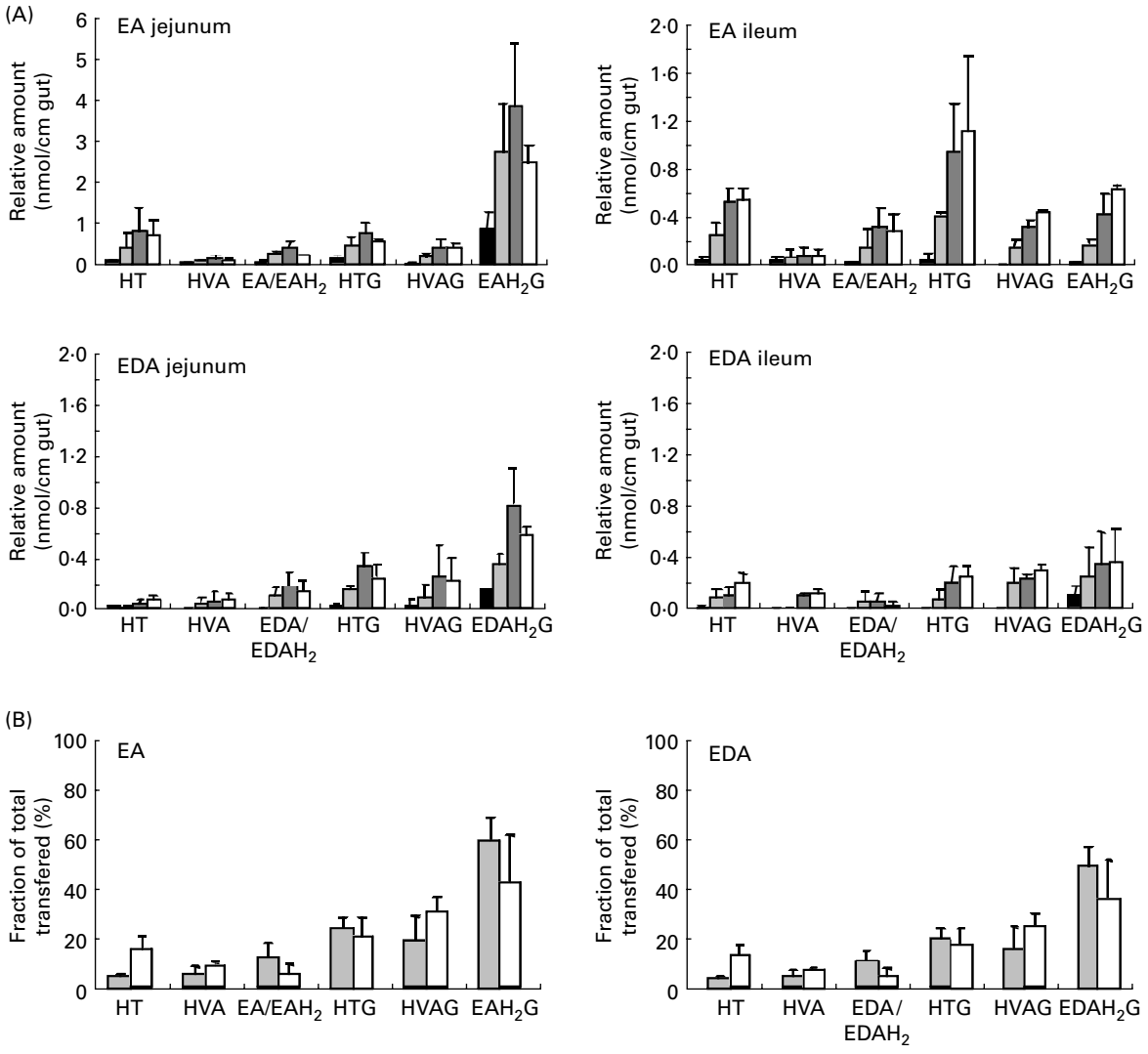

Fig. 8. (A) Cumulative absorption of olive oil polyphenols and their metabolites over 80 min through the isolated rat jejunum and ileum after perfusion with 3,4-dihydroxyphenylethanol-elenolic acid (3,4-DHPEA-EA) and 3,4-dihydroxyphenylethanol-elenolic acid dialdehyde (3,4-DHPEA-EDA). (B) Relative amount of 3,4-DHPEA-EA and 3,4-DHPEA-EDA and their conjugates and metabolites after perfusion through the isolated rat jejunum and ileum. Values are means of at least four separate experiments, with standard errors represented by vertical bars. (A) ■, 20 min; ▒, 40 min; ▓, 60 min; □, 80 min. (B) ▒, Jejunum; □, ileum. HT, hydroxytyrosol; HVA, homovanillyl alcohol; HTG, hydroxytyrosol glucuronides; HVAG, homovanillyl alcohol glucuronides; EAH_2G, glucuronides of the reduced 3,4-DHPEA-EA; $EDAH_2G$, glucuronides of the reduced 3,4-DHPEA-EDA; $EDAH_2$, reduced 3,4-DHPEA-EDA; EAH_2, hydrogenated 3,4-DHPEA-EA.

of the novel metabolites identified in the present study, and those resulting from intestinal micobiota-induced metabolism[23], when investigating biological fluids. Furthermore, such metabolites should be investigated for their cellular and molecular effects in *in vitro* models, as such metabolites may possess biological activities that underpin the benefits of olive oil consumption in humans.

Acknowledgements

We would like to thank the sabbatical grant SFRH/BSAB/877/2008 from FCT and the Treaty of Windsor Anglo-Portuguese Joint Research Programme B15/09 for the financial support. The authors declare that they have no conflicts of interest. J. P. performed the majority of the experimental work; F. P.-M. contributed to the study design, summarised the results and contributed to the manuscript preparation; E. S. D. supervised the experiments with the perfused rat intestinal segments, G. C. coordinated a number of experiments, the HPLC analysis and collaborated on the manuscript preparation; M. J. O.-C. collaborated on the LC–MS analysis and contributed to the manuscript preparation; D. V. and M. H. G. contributed to the cells and HPLC work; J. P. E. S. contributed to the study design and directed interpretation of the results and manuscript preparation. All authors read and approved the final manuscript.

References

1. Sofi F, Abbate R, Gensini GF, *et al.* (2010) Accruing evidence about benefits of adherence to the Mediterranean diet on health: an updated systematic review and meta-analysis. *Am J Clin Nutr* **92**, 1189–1196.
2. Braga C, La Vecchia C, Franceschi S, *et al.* (1998) Olive oil, other seasoning fats, and the risk of colorectal carcinoma. *Cancer* **82**, 448–453.
3. Keys A (1995) Mediterranean diet and public health: personal reflections. *Am J Clin Nutr* **61**, 1321S–1323S.
4. Lopez-Miranda J, Perez-Jimenez F, Ros E, *et al.* (2010) Olive oil and health: summary of the II international conference on olive oil and health consensus report, Jaen and Cordoba (Spain) 2008. *Nutr Metab Cardiovasc Dis* **20**, 284–294.
5. Owen RW, Giacosa A, Hull WE, *et al.* (2000) The antioxidant/anticancer potential of phenolic compounds isolated from olive oil. *Eur J Cancer* **36**, 1235–1247.
6. Owen RW, Haubner R, Wurtele G, *et al.* (2004) Olives and olive oil in cancer prevention. *Eur J Cancer Prev* **13**, 319–326.
7. Montedoro G, Servili M, Baldioli M, *et al.* (1993) Simple and hydrolyzable phenolic compounds in virgin olive oil. 3. Spectroscopic Characterizations of the Secoiridoid Derivatives. *J Agric Food Chem* **41**, 2228–2234.
8. Brenes M, Garcia A, Garcia P, *et al.* (2001) Acid hydrolysis of secoiridoid aglycons during storage of virgin olive oil. *J Agric Food Chem* **49**, 5609–5614.
9. Garcia A, Brenes M, Martinez F, *et al.* (2001) High-performance liquid chromatography evaluation of phenols in virgin olive oil during extraction at laboratory and industrial scale. *J Am Oil Chem Soc* **78**, 625–629.
10. Tovar MJ, Motilva MJ & Romero MP (2001) Changes in the phenolic composition of virgin olive oil from young trees (*Olea europaea* L. cv. Arbequina) grown under linear irrigation strategies. *J Agric Food Chem* **49**, 5502–5508.
11. Paiva-Martins F, Fernandes J, Rocha S, *et al.* (2009) Effects of olive oil polyphenols on erythrocyte oxidative damage. *Mol Nutr Food Res* **53**, 609–616.
12. Paiva-Martins F, Fernandes J, Santos V, *et al.* (2010) Powerful protective role of 3,4-dihydroxyphenylethanol-elenolic acid dialdehyde against erythrocyte oxidative-induced hemolysis. *J Agric Food Chem* **58**, 135–140.
13. Fabiani R, Rosignoli P, De Bartolomeo A, *et al.* (2008) Oxidative DNA damage is prevented by extracts of olive oil, hydroxytyrosol, and other olive phenolic compounds in human blood mononuclear cells and HL60 cells. *J Nutr* **138**, 1411–1416.
14. Garcia-Villalba R, Carrasco-Pancorbo A, Oliveras-Ferraros C, *et al.* (3000) Characterization and quantification of phenolic compounds of extra-virgin olive oils with anticancer properties by a rapid and resolutive LC-ESI-TOF MS method. *J Pharm Biomed Anal* **51**, 416–429.
15. Menendez JA, Vazquez-Martin A, Garcia-Villalba R, *et al.* (2008) tabAnti-HER2 (erbB-2) oncogene effects of phenolic compounds directly isolated from commercial extra-virgin olive oil (EVOO). *BMC Cancer* **8**, 377.
16. Menendez JA, Vazquez-Martin A, Oliveras-Ferraros C, *et al.* (2009) Extra-virgin olive oil polyphenols inhibit HER2 (erbB-2)-induced malignant transformation in human breast epithelial cells: relationship between the chemical structures of extra-virgin olive oil secoiridoids and lignans and their inhibitory activities on the tyrosine kinase activity of HER2. *Int J Oncol* **34**, 43–51.
17. D'Angelo S, Manna C, Migliardi V, *et al.* (2001) Pharmacokinetics and metabolism of hydroxytyrosol, a natural antioxidant from olive oil. *Drug Metab Dispos* **29**, 1492–1498.
18. Miro-Casas E, Covas MI, Farre M, *et al.* (2003) Hydroxytyrosol disposition in humans. *Clin Chem* **49**, 945–952.
19. Miro-Casas E, Covas MI, Fito M, *et al.* (2003) Tyrosol and hydroxytyrosol are absorbed from moderate and sustained doses of virgin olive oil in humans. *Eur J Clin Nutr* **57**, 186–190.
20. Visioli F, Galli C, Bornet F, *et al.* (2000) Olive oil phenolics are dose-dependently absorbed in humans. *FEBS Lett* **468**, 159–160.
21. Vissers MN, Zock PL, Roodenburg AJ, *et al.* (2002) Olive oil phenols are absorbed in humans. *J Nutr* **132**, 409–417.
22. Weinbrenner T, Fito M, Farre Albaladejo M, *et al.* (2004) Bioavailability of phenolic compounds from olive oil and oxidative/antioxidant status at postprandial state in healthy humans. *Drugs Exp Clin Res* **30**, 207–212.
23. Corona G, Tzounis X, Assunta Dessi M, *et al.* (2006) The fate of olive oil polyphenols in the gastrointestinal tract: implications of gastric and colonic microflora-dependent biotransformation. *Free Radic Res* **40**, 647–658.
24. Manna C, Galletti P, Maisto G, *et al.* (2000) Transport mechanism and metabolism of olive oil hydroxytyrosol in Caco-2 cells. *FEBS Lett* **470**, 341–344.
25. Tuck KL, Freeman MP, Hayball PJ, *et al.* (2001) The *in vivo* fate of hydroxytyrosol and tyrosol, antioxidant phenolic constituents of olive oil, after intravenous and oral dosing of labeled compounds to rats. *J Nutr* **131**, 1993–1996.
26. Lipinski CA, Lombardo F, Dominy BW, *et al.* (1997) Experimental and computational approaches to estimate solubility and permeability in drug discovery and development settings. *Adv Drug Deliv Rev* **23**, 3–25.
27. Paiva-Martins F, Gordon MH & Gameiro P (2003) Activity and location of olive oil phenolic antioxidants in liposomes. *Chem Phys Lipids* **124**, 23–36.

28. Limiroli R, Consonni R, Ottolina G, *et al.* (1995) ^{1}H NMR and ^{13}C NMR characterization of new oleuropein aglycones. *J Chem Soc Perkin Trans* **1**, 1519–1523.
29. Paiva-Martins F & Gordon MH (2001) Isolation and characterization of the antioxidant component 3,4-dihydroxyphenylethyl 4-formyl-3-formylmethyl-4-hexenoate from olive (*Olea europaea*) leaves. *J Agric Food Chem* **49**, 4214–4219.
30. Fisher RB & Gardner ML (1974) A kinetic approach to the study of absorption of solutes by isolated perfused small intestine. *J Physiol* **241**, 211–234.
31. Spencer JP, Chowrimootoo G, Choudhury R, *et al.* (1999) The small intestine can both absorb and glucuronidate luminal flavonoids. *FEBS Lett* **458**, 224–230.
32. Paiva-Martins F & Gordon MH (2005) Interactions of ferric ions with olive oil phenolic compounds. *J Agric Food Chem* **53**, 2704–2709.
33. Lenaerts K, Bouwman FG, Lamers WH, *et al.* (2007) Comparative proteomic analysis of cell lines and scrapings of the human intestinal epithelium. *BMC Genomics* **8**, 91.
34. Meunier V, Bourrie M, Berger Y, *et al.* (1995) The human intestinal epithelial cell line Caco-2; pharmacological and pharmacokinetic applications. *Cell Biol Toxicol* **11**, 187–194.
35. Fisher MB, Paine MF, Strelevitz TJ, *et al.* (2001) The role of hepatic and extrahepatic UDP-glucuronosyltransferases in human drug metabolism. *Drug Metab Rev* **33**, 273–297.
36. Gregory PA, Lewinsky RH, Gardner-Stephen DA, *et al.* (2004) Regulation of UDP glucuronosyltransferases in the gastrointestinal tract. *Toxicol Appl Pharmacol* **199**, 354–363.
37. Walgren RA, Karnaky KJ Jr, Lindenmayer GE, *et al.* (2000) Efflux of dietary flavonoid quercetin 4′-beta-glucoside across human intestinal Caco-2 cell monolayers by apical multidrug resistance-associated protein-2. *J Pharmacol Exp Ther* **294**, 830–836.
38. Walgren RA, Lin JT, Kinne RK, *et al.* (2000) Cellular uptake of dietary flavonoid quercetin 4′-beta-glucoside by sodium-dependent glucose transporter SGLT1. *J Pharmacol Exp Ther* **294**, 837–843.
39. Walgren RA, Walle UK & Walle T (1998) Transport of quercetin and its glucosides across human intestinal epithelial Caco-2 cells. *Biochem Pharmacol* **55**, 1721–1727.
40. Poquet L, Clifford MN & Williamson G (2008) Investigation of the metabolic fate of dihydrocaffeic acid. *Biochem Pharmacol* **75**, 1218–1229.
41. Jez JM, Bennett MJ, Schlegel BP, *et al.* (1997) Comparative anatomy of the aldo-keto reductase superfamily. *Biochem J* **326**, (Pt 3), 625–636.
42. Crosas B, Hyndman DJ, Gallego O, *et al.* (2003) Human aldose reductase and human small intestine aldose reductase are efficient retinal reductases: consequences for retinoid metabolism. *Biochem J* **373**, 973–979.
43. Suarez M, Romero MP, Macia A, *et al.* (2009) Improved method for identifying and quantifying olive oil phenolic compounds and their metabolites in human plasma by microelution solid-phase extraction plate and liquid chromatography–tandem mass spectrometry. *J Chromatogr B Analyt Technol Biomed Life Sci* **877**, 4097–4106.

British Journal of Nutrition